

Computed diffusion-weighted imaging for acute pediatric encephalitis/encephalopathy

Acta Radiologica
0(0) 1–7
© The Foundation Acta Radiologica
2019
Article reuse guidelines:
sagepub.com/journals-permissions
DOI: 10.1177/0284185118823335
journals.sagepub.com/home/acr



Yuji Kamata¹ , Yuki Shinohara¹ , Keita Kuya¹,
Yoshiko Tsubouchi², Yoshiaki Saito², Yoshihiro Maegaki²,
Shinya Fujii¹ and Toshihide Ogawa¹

Abstract

Background: Computed diffusion-weighted imaging (DWI) (cDWI) is a computational technique that can be used to calculate a high b-value image from DWI acquired with at least two different lower b-values.

Purpose: To explore the utility of cDWI for the diagnosis of acute pediatric encephalitis/encephalopathy.

Material and Methods: Twenty-two children were enrolled, for whom acquired DWI (aDWI) with $b = 1000$ and 3000 was examined during the acute phase of febrile encephalitis/encephalopathy. For each patient, cDWI was calculated pixel by pixel from aDWI $b = 0$ and 1000 images by using software equipped with a commercially available image viewer. Quantitative assessment was performed by calculating a signal intensity (SI) ratio, defined as the mean SI of the affected lesion/the mean SI at the center of the pons for each image. The Mann–Whitney test was used for statistical analysis of the SI ratios of cDWI $b = 3000$ versus aDWI $b = 1000$ and cDWI $b = 3000$ versus aDWI $b = 3000$. A P value < 0.05 was considered statistically significant.

Results: The SI ratio of cDWI $b = 3000$ images was significantly higher than that of aDWI $b = 1000$ images ($P = 0.0391$), whereas the SI ratio of cDWI $b = 3000$ images was not significantly different from that of aDWI $b = 3000$ images ($P = 0.991$).

Conclusion: cDWI $b = 3000$ is useful for detecting diffusion-restricted lesions in acute pediatric encephalitis/encephalopathy compared to aDWI $b = 1000$ and 3000 . cDWI enables the generation of high b-value images without additional scanning, which will be helpful for sedated pediatric patients in clinical settings.

Keywords

Diffusion-weighted imaging, computed DWI, high b-value DWI, acute encephalopathy, acute encephalitis, pediatric

Date received: 25 September 2018; accepted: 12 December 2018

Introduction

Magnetic resonance imaging (MRI) is an important diagnostic tool for pediatric patients with central nervous system disorders. In particular, diffusion-weighted imaging (DWI) is a well-known MR sequence that enables highly sensitive detection of pediatric acute encephalitis/encephalopathy (1). Acute encephalopathy with biphasic seizures and late reduced diffusion (AESD) is the most common subtype of acute pediatric encephalopathy in Japan (2–7). In patients with AESD, febrile status epilepticus is observed at the onset, followed by transient recovery of consciousness (2–7). A secondary cluster of seizures occurs on days 3–6,

¹Division of Radiology, Department of Pathophysiological and Therapeutic Science, Faculty of Medicine, Tottori University, Yonago, Japan

²Division of Child Neurology, Department of Brain and Neurosciences, Faculty of Medicine, Tottori University, Yonago, Japan

Corresponding author:

Yuji Kamata, Division of Radiology, Department of Pathophysiological and Therapeutic Science, Faculty of Medicine, Tottori University, 36-1 Nishi-cho, Yonago 683-8504, Japan.
Email: xillionec.zillionfw@gmail.com

with MRI showing restricted diffusion in subcortical regions (2–7). Mild encephalopathy with a reversible lesion in the splenium (MERS) is also a relatively common type of acute encephalopathy during childhood and the neurological symptoms completely recover within one month (2,8). The characteristic DWI finding of MERS is a reversible lesion with homogeneously reduced diffusion in the corpus callosum (at least involving the splenium). MERS is sometimes associated with symmetrical white matter lesions (2,8). For neonatal patients with herpes simplex virus encephalitis (HSE), DWI is considered to be more useful for detecting lesions in the cerebral cortex, white matter, basal ganglia, brainstem, and cerebellum compared to other conventional MR sequences (9–11).

Recent technical advances have been made in MRI, including introduction of more sophisticated DWI protocols that are clinically available and that can detect lesions with purely restricted diffusion, e.g. intravoxel incoherent motion imaging (IVIM) (12,13) or acquired DWI (aDWI) with high b-values (14). We previously reported that aDWI of $b = 3000$ is superior to that of $b = 1000$ for the diagnosis of some types of pediatric acute encephalitis/encephalopathy (15).

Computed DWI (cDWI) is a computational technique that can be used to calculate a high b-value (or any b-value) image from DWI acquired with at least two different lower b-values (16). Therefore, a DWI with a hypothetical high b-value can be obtained without additional scanning of the patient. According to previous studies, cDWI enables acquisition of high b-value images with superior signal-to-noise ratios (SNR) compared to conventionally acquired DWI (16). Several articles have described the usefulness of cDWI in clinical situations. Blackledge et al. found that cDWI with high b-values enables acquisition of high-quality images with good background signal suppression and malignant lesion conspicuity in their small cohort of cancer patients (16). In another study, Ueno et al. reported that cDWI with $b = 2000$ is superior to aDWI with $b = 1000$ for detecting prostate cancer (17).

The purpose of this study was to clarify the usefulness of cDWI with $b = 3000$ for detecting lesions in acute pediatric encephalitis/encephalopathy compared to that of aDWI with $b = 1000$ and 3000 . To the best of our knowledge, no reports are available on the effectiveness of cDWI with a high b-value in pediatric patients with acute encephalitis/encephalopathy.

Material and Methods

Patients

We reviewed the medical records and MRI of children who were admitted to our institution between August

2008 and July 2015 and for whom high b-value DWI was performed for the brain with a suspicion of serious acute etiologies. Among the 49 eligible individuals, the final diagnosis of 27 patients was febrile convulsion ($n = 15$), epilepsy ($n = 4$), and others ($n = 8$). The remaining 22 patients (11 boys, 11 girls; mean age = 40.8 months; age range = 20 days–126 months) were diagnosed with AESD ($n = 6$), MERS ($n = 6$), unclassifiable acute encephalitis/encephalopathy ($n = 2$), HSE ($n = 3$), acute encephalitis with refractory and repetitive partial seizures (AERRPS; $n = 1$), other encephalopathy ($n = 1$), infarction ($n = 1$), head injury ($n = 1$), or mitochondrial myopathy, encephalopathy, lactic acidosis, and stroke-like episodes (MELAS, $n = 1$). These 22 children were enrolled for further analyses. They are the same cohort as described in our previous study (15). Our institutional review board approved this study and waived the need for written informed consent because of its retrospective design.

Imaging examinations

MR examinations were performed on days 1–26 of the illness in the 22 patients. MRI was performed using one of three 3-T MR systems (Discovery MR750w or Signa EXCITE HD, GE Healthcare, Milwaukee, WI, USA and Magnetom Skyra, Siemens, Munich, Germany). The scan protocol for each DWI was as follows: Discovery MR750w: TR = 7000 ms; TE = 78 ms; field of view (FOV) = 21 cm; matrix = 128×128 ; slice thickness = 5.0 mm; acquisition time = 56 s for $b = 1000$ and TR = 7000 ms; TE = 101 ms; FOV = 21 cm; matrix = 128×128 ; slice thickness = 5.0 mm; acquisition time = 56 s for $b = 3000$; Signa EXCITE HD: TR = 7000 ms; TE = 70 ms; FOV = 21 cm; matrix = 128×128 ; slice thickness = 5.0 mm; acquisition time = 56 s for $b = 1000$ and TR = 7000 ms; TE = 100 ms; FOV = 21 cm; matrix = 128×128 ; slice thickness = 5.0 mm; acquisition time = 56 s for $b = 3000$; Magnetom Skyra: TR = 4520 ms; TE = 53 ms; FOV = 21 cm; matrix = 128×128 ; slice thickness = 5.0 mm; acquisition time = 1 min 26 s for $b = 1000$ and TR = 5140 ms; TE = 77 ms; FOV = 21 cm; matrix = 128×128 ; slice thickness = 5.0 mm; acquisition time = 1 min 38 s for $b = 3000$.

The apparent diffusion coefficient (ADC) is calculated with the equation $ADC = \ln[-S_1/S_0]/(b_1 - b_0)$, using two aDWI signals, S_0 and S_1 , based on a mono-exponential model. Once the ADC is known, the cDWI signal at $b = b_c$ can be obtained with the equation $S_c = S_0 \exp[-(b_c - b_0)ADC]$ (16). In this study, cDWI $b = 3000$ was generated pixel by pixel from the aDWI $b = 0$ and 1000 images for each patient with software equipped with a commercially available

image viewer (EV Insite; PSP Corporation, Tokyo, Japan).

Qualitative analysis

Visual assessment of cDWI $b=3000$ and aDWI $b=3000$ findings compared to aDWI $b=1000$ findings was performed independently by the consensus of two neuroradiologists (YS and KK with 14 and seven years of experience, respectively). Although these readers were informed of the DWI sequences (cDWI $b=3000$, aDWI $b=3000$, or aDWI $b=1000$) when they evaluated, they were blinded to the clinical information. cDWI $b=3000$, aDWI $b=3000$, and aDWI $b=1000$ images at identical slice levels of the lesions on aDWI $b=3000$ images were presented side by side on a monitor. The two neuroradiologists defined aDWI $b=3000$ or cDWI $b=3000$ images as “significant” if the visibility of the affected lesions on each sequence was superior to aDWI $b=1000$. Meanwhile, the readers defined aDWI $b=3000$ or cDWI $b=3000$ images as “insignificant” if the visibility of the affected lesions on each sequence was equal or inferior to aDWI $b=1000$. Statistical analyses regarding the relationship between each sequence (aDWI $b=3000$ versus aDWI $b=1000$ or cDWI $b=3000$ versus aDWI $b=1000$) and its visibility (significant or insignificant) were performed using Fisher’s exact test. A P value < 0.05 was considered statistically significant.

Quantitative analysis

aDWI $b=3000$ image was referenced to the aDWI $b=1000$ image in each case and segmented ROIs were semi-automatically placed in the most obvious high intensity lesion on cDWI $b=3000$ images determined by one neuroradiologist (YS with 14 years of experience). In general, the lesion in pons is unusual in the pediatric acute encephalopathy/encephalitis and our cohort did not show pontine lesions either (15). Therefore, a circular ROI was manually placed in the center of the pons at the level of the middle cerebellar peduncle as a reference. Both ROIs in the affected lesion and the pons on cDWI $b=3000$ images were copied to the transformed aDWI $b=3000$ and aDWI $b=1000$ images (Fig. 1). The signal intensity (SI) ratio for the affected lesion was defined as the mean SI of the affected lesion/the mean SI of the pons. These ROI analyses were performed with a semi-automated commercially available image analysis program (AnalyzePro; Biomedical Imaging Resource, Mayo Foundation, Rochester, MN, USA). We compared the SI ratio of cDWI $b=3000$ with those of aDWI $b=1000$ and aDWI $b=3000$. The Mann–Whitney U test was used for statistical analysis of the SI ratios of

cDWI $b=3000$ versus aDWI $b=1000$ and cDWI $b=3000$ versus aDWI $b=3000$. A P value < 0.05 was considered statistically significant. All calculations were performed with EZR (version 1.35; Saitama Medical Centre, Jichi Medical University), which is a graphical user interface for R (18).

Results

In the qualitative analysis, aDWI $b=3000$ was superior to aDWI $b=1000$ regarding the visibility of affected lesions in all 22 patients. In addition, cDWI $b=3000$ was superior to aDWI $b=1000$ in 19 out of 22 patients; the other three patients showed the same visibility on both cDWI $b=3000$ and aDWI $b=1000$. On the other hand, no statistically significant difference was observed between the visibility of high SI in the affected lesion (significant or insignificant) and the difference in the sequences (aDWI $b=3000$ or cDWI $b=3000$) ($P=0.233$). For quantitative analysis, the SI ratio of cDWI $b=3000$ (median = 1.85) was significantly higher than that of aDWI $b=1000$ (median = 1.41, $P=0.039$, Fig. 2), whereas the SI ratio of cDWI $b=3000$ was not significantly different from that of aDWI $b=3000$ (median = 1.90, $P=0.991$, Fig. 3). The SI ratio for aDWI $b=1000$, aDWI $b=3000$, and cDWI $b=3000$ in each subtype was as follows: 2.00, 3.40, and 4.17 in AESD (median, $n=6$); 1.18, 1.50, and 1.56 in MERS (median, $n=6$); 1.28, 1.69, and 1.63 in unclassifiable acute encephalitis/encephalopathy (median, $n=2$); 1.39, 1.63, and 1.56 in HSE (median, $n=3$); 1.24, 1.92, and 3.19 in AERRPS ($n=1$); 1.49, 2.23, and 1.39 in other encephalopathy ($n=1$); 1.31, 1.39, and 1.76 in infarction ($n=1$); 4.14, 9.63, and 9.13 in head injury ($n=1$); 1.87, 2.00, and 1.86 in MELAS ($n=1$). Case examples are shown in Fig. 4.

Discussion

In our study, cDWI $b=3000$ was significantly superior to aDWI $b=1000$ for visualizing restricted diffusion in acute pediatric encephalitis/encephalopathy. Quantitative analysis also showed that the lesion-to-pons SI ratio of cDWI $b=3000$ images was significantly higher than that of aDWI $b=1000$ images, although no significant difference was seen between the lesion-to-pons SI ratio in cDWI $b=3000$ images and that of aDWI $b=3000$ images. Our previous report indicated the utility of high b -value DWI in pediatric patients with acute encephalitis/encephalopathy in which images were acquired by performing additional scanning of a high b -value sequence (about 1- or 2-min acquisition time in our institution) that we have termed acquired DWI $b=3000$ in this study (15). Our results indicate that cDWI enables the accurate

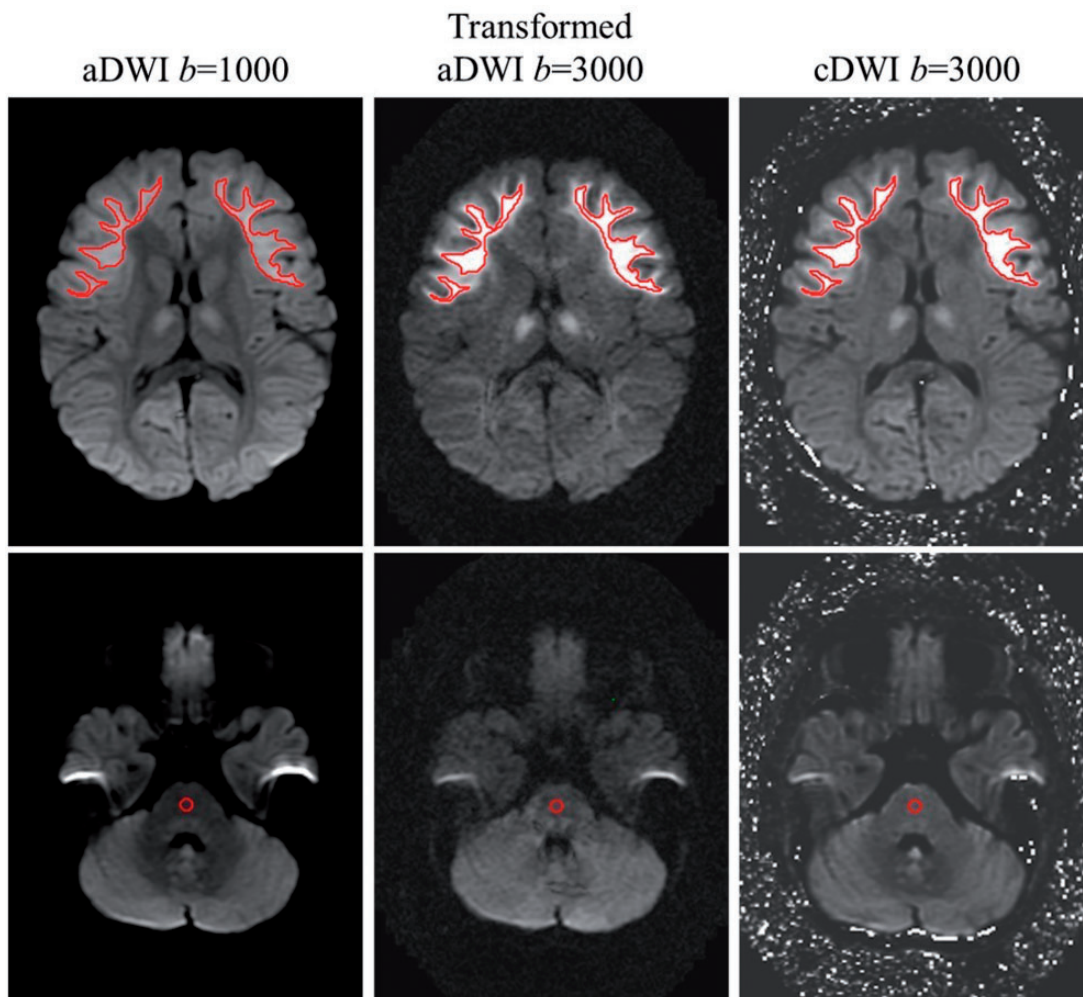


Fig. 1. A 23-month-old girl with AESD on day 4 of the illness. Segmented ROIs are placed in the most obvious high intensity lesion on cDWI $b=3000$ images and a circular ROI is placed in the center of the pons at the level of the middle cerebellar peduncle as a reference. Both ROIs are copied to the transformed aDWI $b=3000$ and aDWI $b=1000$ images.

diagnosis of acute pediatric encephalitis/encephalopathy by obtaining a high b-value DWI, which does not require additional scanning. Although a safe and appropriate sedation is required to obtain MR images with high quality in the pediatric patients, potential risks of anesthesia have been also well known (19, 20). Because shortening of the MR examination time is highly desirable in sedated pediatric patients, this imaging sequence will be helpful for such patients in the clinical setting. In addition, radiologists can obtain and evaluate high b-value DWI retrospectively even after the examination by applying cDWI technique, so long as the patients have undergone conventional MR examination including $b=0$ and 1000 DWIs.

Several studies have reported that DWI with a high b-value is useful for the diagnosis of certain central

nervous system disorders. Although controversy exists regarding whether a high b-value is effective for detecting restricted diffusion in patients with acute ischemic stroke, in other conditions, Seo et al. has reported that DWI $b=3000$ is more useful than DWI $b=1000$ for differentiating between high- and low-grade gliomas at 3 T (14). In addition to our previous report on the utility of high b-value DWI in acute pediatric encephalitis/encephalopathy (15), Tachibana et al. has also reported that the ability to detect slight changes in cortical and subcortical lesions in acute encephalopathy may be superior in a fraction of high b-pair maps compared to ADC (21).

cDWI is a computational technique that can produce images with any b-value from DWI acquired with at least two different b-values (16). Thus, cDWI software is a post-processing tool that allows the

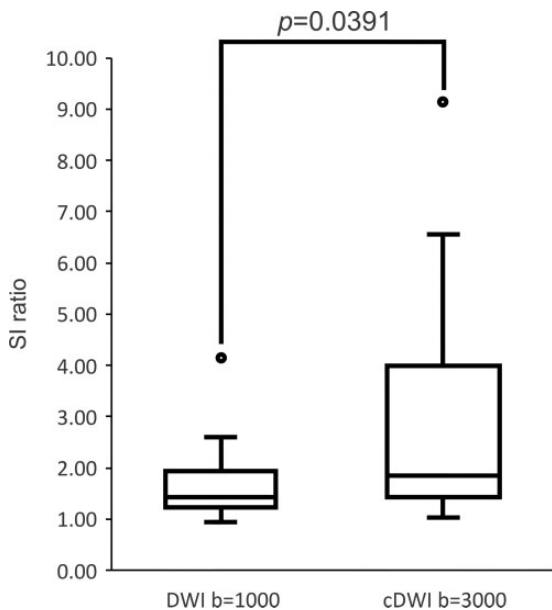


Fig. 2. Difference in the signal intensity (SI) ratio between acquired DWI (aDWI) b=1000 and computed DWI (cDWI) b=3000. The SI ratio of cDWI b=3000 (median = 1.85) is significantly higher than that of aDWI b=1000 (median = 1.41) ($P = 0.0391$).

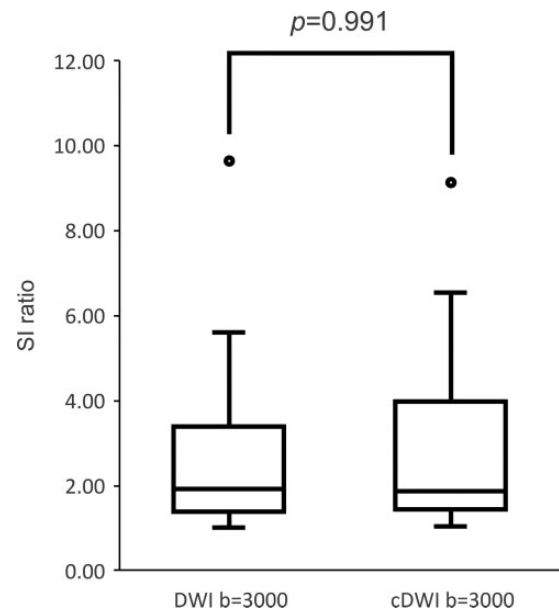


Fig. 3. Difference in the signal intensity (SI) ratio between b=3000 acquired DWI (aDWI) and computed DWI (cDWI). The SI ratio of cDWI b=3000 (median = 1.85) is not significantly different from that of aDWI b=3000 (median = 1.90) ($P = 0.991$).

reconstruction of DWIs at any b-value after the MR examinations (16,17). Some articles have indicated that high b-value images generated using cDWI can improve detection of tumors such as prostate cancer, breast cancer, malignant lymphoma, and hepatic metastases (16,17,22). To the best of our knowledge, no reports are available about the utility of cDWI for central nervous system disorders including pediatric brain diseases. This is the first study that shows the utility of high b-value images derived from the cDWI technique in pediatric patients with acute encephalitis/encephalopathy.

According to previous articles on tumor detection using cDWI, cDWI enables high-sensitivity detection of diffusion-restricted lesions because of both the feasible acquisition of higher b-values images and the good SNR due to background noise suppression with concomitant maintenance of the original lesion signal (16,17). However, the optimization of cDWI has been controversial. In accordance with a previous article, the cDWI theory in our study was similarly based on calculating the ADC with a mono-exponential model (17). However, in one article, the authors suggested that a more complex model for cDWI will be needed in clinical settings (21), whereas others have reported the usefulness of a bi-exponential model including intravoxel incoherent motion MR imaging for detecting diffusion-

restricted lesions (12,13,24,25). Furthermore, other sets of b-values or computed high b-values may be better for depicting reduced diffusion in patients with acute encephalitis/encephalopathy, although in our study, we fixed the two b-values at b=0 and 1000 and only assessed cDWI b=3000. Because our study was relatively preliminary, further investigation is required to optimize cDWI in pediatric patients with acute encephalitis/encephalopathy.

This study has several limitations. First, this study was retrospective and vulnerable to selection and verification biases. Second, only a small number of patients was enrolled. Third, there is broad variation in the period between onset and MRI (1–26 days) during the acute illness. Lastly, differences in cDWI findings among each subgroup, such as AESD, MERS, and HSE, could not be evaluated. As each disease likely has its own pathophysiological mechanism, the cDWI finding of each disease may consequently be different. Therefore, additional studies should be performed in the future.

In conclusion, cDWI with b=3000 is useful for detecting diffusion-restricted lesions in acute pediatric encephalitis/encephalopathy compared to aDWI with b=1000 and b=3000. cDWI enables high b-value images to be generated without additional scanning of the patient, which shortens the MR examination

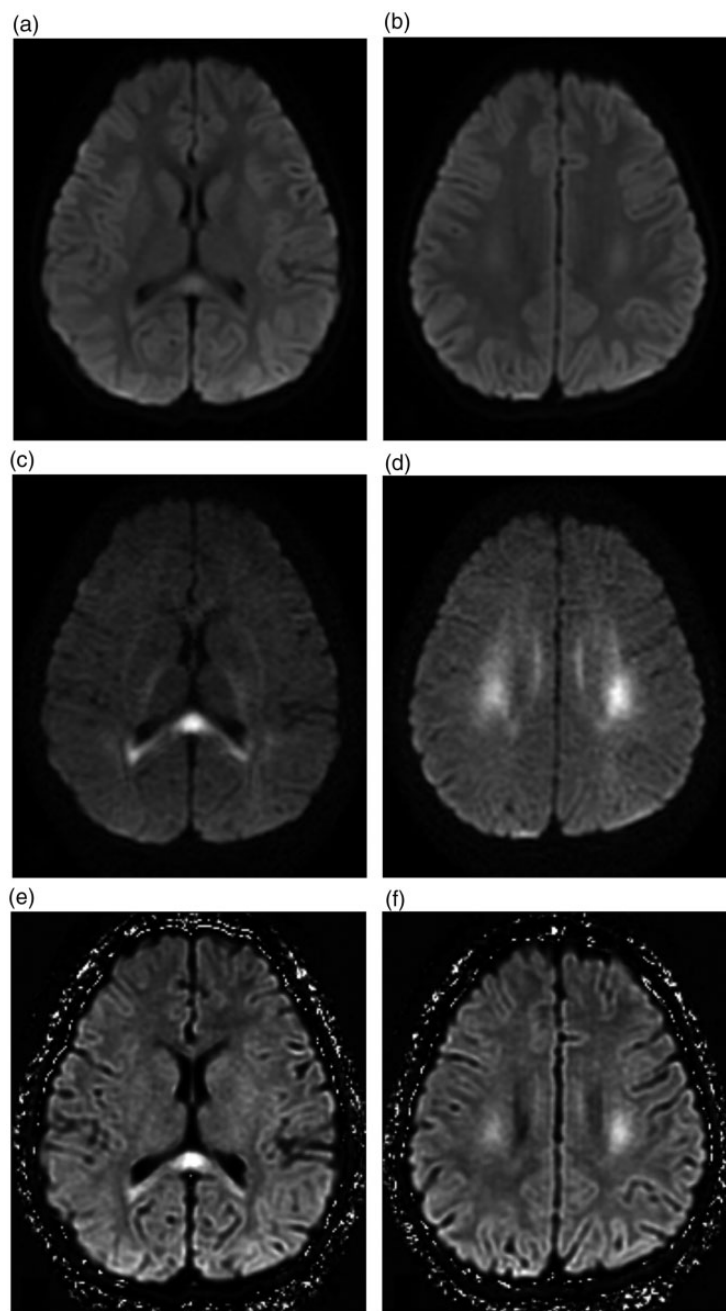


Fig. 4. MRI of a 73-month-old boy with mild encephalopathy with reversible lesions in the splenium type 2 on day 5 of the illness. (a, b) Acquired DWI (aDWI) $b = 1000$, (c, d) aDWI $b = 3000$, (e, f) cDWI $b = 3000$. cDWI $b = 3000$ (e, f) and aDWI $b = 3000$ (c, d) show higher signal intensity in the splenium of the corpus callosum and bilateral centrum semiovale compared to that of aDWI $b = 1000$ (a, b).

time and would therefore be helpful for sedated pediatric patients in clinical settings.

Declaration of conflicting interests


The authors declared no potential conflicts of interest with respect to the research, authorship, and/or publication of this article.

Funding

The authors received no financial support for the research, authorship, and/or publication of this article.

ORCID iD

Yuji Kamata  <http://orcid.org/0000-0002-9128-690X>

Yuki Shinohara  <http://orcid.org/0000-0001-6586-4086>

References

1. Utsunomiya H. Diffusion MRI abnormalities in pediatric neurological disorders. *Brain Dev* 2011;33:235–242.
2. Takanashi J. Two newly proposed infectious encephalitis/encephalopathy syndromes. *Brain Dev* 2009;31:521–528.
3. Maegaki Y, Kondo A, Okamoto R, et al. Clinical characteristics of acute encephalopathy of obscure origin: a biphasic clinical course is a common feature. *Neuropediatrics* 2006;37:269–277.
4. Takanashi J, Oba H, Barkovich AJ, et al. Diffusion MRI abnormalities after prolonged febrile seizures with encephalopathy. *Neurology* 2006;66:1304–1309.
5. Mizuguchi M, Yamanouchi H, Ichiyama T, et al. Acute encephalopathy associated with influenza and other viral infections. *Acta Neurol Scand* 2007;115:45–56.
6. Takanashi J, Tada H, Terada H, et al. Excitotoxicity in acute encephalopathy with biphasic seizures and late reduced diffusion. *Am J Neuroradiol* 2009;30:132–135.
7. Kuya K, Fujii S, Miyoshi F, et al. A case of acute encephalopathy with biphasic seizures and late reduced diffusion: Utility of arterial spin labeling sequence. *Brain Dev* 2017;39:84–88.
8. Tada H, Takanashi J, Barkovich AJ, et al. Clinically mild encephalitis/encephalopathy with a reversible splenic lesion. *Neurology* 2004;63:1854–1858.
9. Vossough A, Zimmerman RA, Bilaniuk LT, et al. Imaging findings of neonatal herpes simplex virus type 2 encephalitis. *Neuroradiology* 2008;50:355–366.
10. Teixeira J, Zimmerman RA, Haselgrove JC, et al. Diffusion imaging in pediatric central nervous system infections. *Neuroradiology* 2001;43:1031–1039.
11. Okanishi T, Yamamoto H, Hosokawa T, et al. Diffusion-weighted MRI for early diagnosis of neonatal herpes simplex encephalitis. *Brain Dev* 2015;37:423–431.
12. Le Bihan D, Breton E, Lallemand D, et al. MR imaging of intravoxel incoherent motions: application to diffusion and perfusion in neurologic disorders. *Radiology* 1986;161:401–407.
13. Le Bihan D, Breton E, Lallemand D, et al. Separation of diffusion and perfusion in intravoxel incoherent motion MR imaging. *Radiology* 1988;168:497–505.
14. Seo HS, Chang KH, Na DG, et al. High b-value diffusion ($b=3000$ s/mm²) MR imaging in cerebral gliomas at 3T: visual and quantitative comparisons with $b=1000$ s/mm². *Am J Neuroradiol* 2008;29:458–463.
15. Tsubouchi Y, Itamura S, Saito Y, et al. Use of high b value diffusion-weighted magnetic resonance imaging in acute encephalopathy/encephalitis during childhood. *Brain Dev* 2018;40:116–125.
16. Blackledge MD, Leach MO, Collins DJ, et al. Computed diffusion-weighted MR imaging may improve tumor detection. *Radiology* 2011;261:573–581.
17. Ueno Y, Takahashi S, Kitajima K, et al. Computed diffusion-weighted imaging using 3-T magnetic resonance imaging for prostate cancer diagnosis. *Eur Radiol* 2013;23:3509–3516.
18. Kanda Y. Investigation of the freely available easy-to-use software ‘EZR’ for medical statistics. *Bone Marrow Transplant* 2013;48:452–458.
19. American Academy of Pediatrics, American Academy of Pediatric Dentistry, Coté CJ, et al. Guidelines for monitoring and management of pediatric patients during and after sedation for diagnostic and therapeutic procedures: an update. *Pediatrics* 2006;118:2587–2602.
20. Jaimes C, Gee MS. Strategies to minimize sedation in pediatric body magnetic resonance imaging. *Pediatr Radiol* 2016;46:916–927.
21. Tachibana Y, Aida N, Niwa T, et al. Analysis of multiple b-value diffusion-weighted imaging in pediatric acute encephalopathy. *PLoS One* 2013;8:e63869.
22. Shimizu H, Isoda H, Fujimoto K, et al. Comparison of acquired diffusion weighted imaging and computed diffusion weighted imaging for detection of hepatic metastases. *Eur J Radiol* 2013;82:453–458.
23. Kimura T, Machii Y. Computed diffusion weighted imaging under rician noise distribution [abstr]. In: *Proceedings of the International Society for Magnetic Resonance in Medicine*. Berkeley, CA: International Society for Magnetic Resonance in Medicine 2012:3574.
24. Riches SF, Hawtin K, Charles-Edwards EM, et al. Diffusion-weighted imaging of the prostate and rectal wall: comparison of biexponential and monoexponential modelled diffusion and associated perfusion coefficients. *NMR Biomed* 2009;22:318–325.
25. Yamada I, Aung W, Himeno Y, et al. Diffusion coefficients in abdominal organs and hepatic lesions: evaluation with intravoxel incoherent motion echo-planar MR imaging. *Radiology* 1999;210:617–623.